

**On the relation between interstellar spectral features and reddening**

Krełowski, J.

Center for Astronomy, Nicholas Copernicus University, Gagarina 11, Pl-87-100 Toruń,  
Poland  
Rzeszów University, al. T. Rejtana 16c, 35-959 Rzeszów, Poland  
e-mail: jacek@astri.uni.torun.pl

Galazutdinov, G.

Instituto de Astronomia, Universidad Catolica del Norte, Av. Angamos 0610, Antofagasta,  
Chile  
Pulkovo Observatory, Pulkovskoe Shosse 65, Saint-Petersburg, Russia  
Special Astrophysical Observatory, Nizhnij Arkhyz, 369167, Russia  
e-mail: runizag@gmail.com

Godunova, V.

ICAMER Observatory, NAS of Ukraine, 27 Acad. Zabolotnoho Str., 03143, Kyiv, Ukraine  
e-mail: v\_godunova@bigmir.net

Bondar, A.

ICAMER Observatory, NAS of Ukraine, 27 Acad. Zabolotnoho Str., 03143, Kyiv, Ukraine  
e-mail: arctur.ab@gmail.com

## ABSTRACT

It is well known that interstellar spectral features correlate with color excess  $E(B - V)$ . This suggests that measuring intensities of these features allows one to estimate reddening of stars. The aim of this paper is to check how tight intensities of interstellar diffuse bands (DIBs) are related to the amount of extinction, measured using  $E(B - V)$ .

We have measured equivalent widths of the strongest DIBs (centered at  $\lambda\lambda$  5780.6, 5797.0, 6196.0, 6379.3, 6613.5, and 8620.7 Å), as well as of CH (near 4300.3 Å) and CH<sup>+</sup> (near 4232.5 Å) in high resolution, high S/N ratio echelle spectra from several spectrographs. The equivalent widths of the 8620 DIB in noisy spectra were measured using a template, which was constructed using the high quality spectrum of BD+40 4220. DIB relations with the color excess in the range 0.1–2.0 mag were examined. Our careful analysis demonstrates that all the above mentioned interstellar spectral features (except, perhaps, 6379 DIB) do correlate with  $E(B - V)$  relatively tightly (with the Pearson's correlation coefficient of 0.8+). Moreover, the observed scatter is apparently not caused by

measurement errors but is of physical origin. We present several examples where the strength ratios of a DIB/molecule to  $E(B - V)$  are different than the average.

**Key words:** *ISM: clouds – ISM: dust, extinction: ISM: molecules – lines and bands*

## 1. Introduction

Absorption features, originating in translucent interstellar clouds, are being revealed due to the presence of the following non-stellar phenomena in spectra of reddened OB stars:

- Interstellar extinction, usually known as *reddening*, which selectively attenuates starlight. It is commonly believed to be caused by some solid particles of submicron size; however, since the beginning of investigations of this phenomenon (Trumpler, 1930) some neutral (gray) extinction, caused by relatively large dust particles, was proposed as well.
- Polarization – also believed to be caused by dust particles when the latter are non-spherical and oriented by e.g. magnetic field.
- Spectral lines of interstellar atomic gas, e.g., *H* and *K* doublet of CaII, discovered by Hartmann (1904). The survey of UV interstellar lines (Field, 1974) proved that heavy elements in the ISM are strongly depleted in comparison to their abundances in stellar atmospheres, likely because of dust formation out of heavy elements and of chemical reactions leading to the formation of different (possibly complex) molecules.
- Molecular bands of simple radicals (CH, OH, NH, CN, C<sub>2</sub>, C<sub>3</sub>, OH<sup>+</sup>, SH), some of them were discovered and identified long ago (McKellar 1941). Since the 1970s, rotational emission features revealed the presence in the star forming regions of many complex (currently ~200) molecules with a dipole momentum;
- Diffuse interstellar bands (DIBs): their identification is the longest standing unsolved problem of the spectroscopy in general. The first two such features were discovered in 1921 by Heger (1922). The application of solid state detectors to DIB observations led to discoveries of new features. Currently, the list of known DIBs exceeds 500 entries (Galazutdinov et al., 2000, Hobbs et al., 2008, Fan et al., 2019); a majority of them are very shallow. Even more importantly, the fine structure (reminiscent of the rotational structure of polyatomic molecules) has been detected in most of narrow DIBs (Kerr et al. 1998). Nearly all conceivable forms of matter – from hydrogen anion to dust grains – have already been proposed as DIB carriers, so far with no generally accepted success. It should be noted that their variable strength ratios suggest a variety of carriers, and thus strongly support their molecular

origin (for review, see Krelowski (2018)). Publications of Campbell et al. (2015, 2016, 2016a) re-started the discussion on whether  $C_{60}^+$  molecule may carry strong near-infrared spectral features of interstellar origin seen at 9633 and 9577 Å. Galazutdinov et al. (2017a, 2017b) disputed the identifications, pointing out the problem of the variable strength ratio of these two strong features. The problem of variable strength ratio remains unsolved also after the recent publication of Cordiner et al. (2019) based on HST spectra free of telluric contamination but not covering the 9633 DIB.

As evidenced by Fitzpatrick and Massa (2007), it seems well-established that interstellar absorption spectra, in particular extinction curves, may differ from cloud to cloud. Sneden, Woszcyk & Krelowski (1991) proposed already a division of interstellar clouds into  $\sigma$  and  $\zeta$  type objects. The interstellar spectra of such objects are different showing variable strength ratios of molecular/atomic/diffuse features. In general diffuse bands intercorrelations are tight. These were recently demonstrated by Bailey et al. (2016) who confirmed earlier results of Moutou et al. (1999). Bailey et al. (2016) demonstrated also that in nearby, single cloud lines-of-sight often these correlations weaken that results from observing  $\sigma$  and  $\zeta$  type objects alone. Tight correlations follow usually adding up several clouds. However, having spectra of high enough resolution and S/N ratio, one can resolve individual Doppler components in interstellar atomic and/or molecular lines. In cases of diffuse bands, it is very difficult and possible only in very specific occasions. When dealing with extinction and polarization it is absolutely impossible. Since the extinction and polarization curves may change when sightlines intersect several clouds (in particular, the light beam may get depolarised by a subsequent cloud), the only possibility to investigate these phenomena in relation to other ones, is to observe stars when interstellar atomic/molecular lines do not show any Doppler splitting. Such objects are relatively scarce and may be found only by means of high resolution spectral observations. High resolution echelle spectra can not only allow one to distinguish between single and multiple cloud cases. As already suggested (Sneden, Woszcyk & Krelowski, 1991), also the linear polarization of interstellar spectra may vary together with the shape of the extinction curve.

Amount and characteristics of dust vary greatly from one interstellar cloud to another that poses difficulties in constructing the distance scale in the Galaxy (e.g. Fitzpatrick & Massa (2007), Siebenmorgen et al. (2014), etc). In fact, distant objects may be reddened either by one or more translucent interstellar clouds situated along the lines of sight towards them. Knowledge of distances to cosmic objects is of basic importance for investigating their physical properties, including absolute stellar magnitude. However, the latter can be reciprocally used for distance estimation if being properly calibrated to the spectrum and luminosity class of an observed object.

The most popular measure of extinction (reddening) is the color excess  $E(B - V) = A_B - A_V = (B - V)_{obs} - (B - V)_o$ , where  $(B - V)_{obs}$  is an object's observed

color index, and  $(B - V)_o$  is its intrinsic value, whereas  $A_B$  and  $A_V$  are the total extinctions in the photometric  $B$  (4400 Å) and  $V$  (5500 Å) bands, respectively. Another measure of extinction is the absolute extinction  $A = A_\lambda/A_V$ , where  $A_\lambda$  is the total extinction at wavelength  $\lambda$ . As a rule, color excess grows with increasing absolute extinction.

Extinction effects (e.g. reddening) are most often observed in spectra of early-type stars due to their high intrinsic brightness, which allows one to observe distant, heavily reddened objects. Extinction has for a very long time been considered to be correlated with spectral features of interstellar origin, in particular with DIBs, which are best seen especially towards the above mentioned early-type objects (of spectral types O or B) strongly radiating in the optical region with relatively few purely stellar absorption features.

Years ago, Merrill & Wilson (1938) established the presence of the correlation between the 6284 DIB and color excess. Later Greenstein & Aller(1950) demonstrated a similar effect for the strongest DIB centered at  $\lambda$  4430 Å. An extensive examination of eight DIBs and their correlations was performed by Friedman et al.(2011). Furthermore, behavior of interstellar features in spectra of reddened stars was a subject of intent scientific research by Friedman et al.(2011), Kashuba et al.(2016), York et al.(2014). New, infrared DIBs have recently been described by Hamano et al.(2016), Galazutdinov et al.(2017a). For a recent review see Krelowski (2018). Results of these and other studies may suggest application of interstellar features, such as diffuse interstellar bands, to estimate color excesses and, consequently, total extinction.

## 2. Investigations of the 8620 DIB as a spectroscopic tracer of extinction

The diffuse interstellar band at  $\lambda$  8620.7 Å (the so-called “Gaia DIB”) belongs evidently to the class of reasonably broad features. It is the only unambiguous DIB in the wavelength range 8450 – 8720 Å of the Radial Velocity Spectrometer (RVS) aboard Gaia ([www.cosmos.esa.int/web/gaia](http://www.cosmos.esa.int/web/gaia)).

For another similar one (at  $\lambda$  5780.6 Å; a bit narrower than the 8620 one) Krelowski & Westerlund(1988) proved that the DIB intensity can change by a factor of 3 with the same  $E(B - V)$  while comparing spectra of two bright stars:  $\sigma$  Sco and  $\zeta$  Oph (see Fig. 1 of Krelowski & Westerlund(1988)). This led to the division of translucent interstellar clouds into  $\sigma$  and  $\zeta$  cases being now in common use. A considerable growth in the number of studies of the 8620 DIB and its correlation with reddening has been specifically driven by the Gaia space mission. We provide here a short overview of some recently published works. Wallerstein et al.(2007) measured the equivalent width (EW) of this DIB in spectra of 64 stars (recorded with different resolutions) with color excesses of up to 3.17 mag and found a relatively good correlation between the 8620 DIB intensity and  $E(B - V)$ . However, the lack of the EW errors reduces the significance of the reported conclusions. The

method of equivalent width measurements does not bear scrutiny either: “equivalent widths of the DIBs and KI were measured via Gaussian fits to the observed line profiles” (page 1272). It is important to underscore that the Gaussian fit is not well applicable for irregular profiles of diffuse bands. Moreover, Wallerstein et al. used in many cases compilations of measurements, done by somebody else. This creates additional uncertainties as different researchers set continua over DIBs in different fashions. Such averages suffer an excessive scatter which reduces the significance of the results.

Munari et al.(2008) proposed to use the 8620 DIB as a tool to measure the amount of reddening. The equivalent width of this DIB seems (according to Munari et al.) to correlate very tightly with  $E(B - V)$  as seen in Fig. 2 of Munari et al.(2008). However, it is of interest to consider how certain is the  $E(B - V)$  estimate based on the  $EW(8620)$  intensity? Indeed, Munari’s relation is based on the 76 low resolution ( $R=7500$ ) and relatively low  $S/N$  ratio (as low as 50 only) spectra of 68 stars. This may smear out some local differences that makes the relation uncertain.

Kos et al.(2013) confirmed the general correlation between the equivalent width of the 8620 DIB and the reddening in a rather statistical way where both the equivalent width and the reddening magnitude were estimated for a group of targets in a certain volume instead of individual estimations. In the next paper Kos et al.(2014) combined information from nearly 500,000 stellar spectra obtained by the massive spectroscopic survey RAVE to produce a pseudo-3D map of the strength of the 8620 DIB covering the nearest 3 kpc from the Sun, and showed that the 8620 DIB carrier has a significantly larger vertical scale height than the dust. It should be noted that the method applied and the quality of the analyzed data ( $R=7500$  with low  $S/N$  ratio) can provide very general conclusions only.

Maíz Apellániz et al.(2015) studied three objects in the Berkeley 90 cluster. The authors applied the Gauss fit method to measure the equivalent width of the 8620 DIB. As a result, the following conclusion was drawn: “DIB  $\lambda$  8621.20 Å, present in the Gaia band, is a good example of a strong DIB that is expected to correlate poorly with extinction because it appears to be highly depleted in the dense ISM”. However, the low resolution as well as the quality of their spectra make the conclusions uncertain. In particular, low resolution does not allow to distinguish with certainty different Doppler components. Damineli et al.(2016) measured the equivalent width of the 8620 DIB using low resolution spectra ( $R \leq 15000$ ) obtained for 11 bright members from the Westerlund 1 stellar cluster and for 12 objects along other Galactic directions. The authors derived a relation  $EW(8620)$  vs.  $E(B - V)$ , which extends Munari et al.(2008)’s relation to the non-linear regime ( $A_V \geq 4$  mag).

The Gaia DIB is situated in the wavelength range populated with the hydrogen Paschen lines. In B type spectra one can also observe lines of helium and some other elements, as shown in Fig. 1. This plot demonstrates also that the 8648 DIB, mentioned by Jenniskens & Desert (1994), is most probably a stellar helium

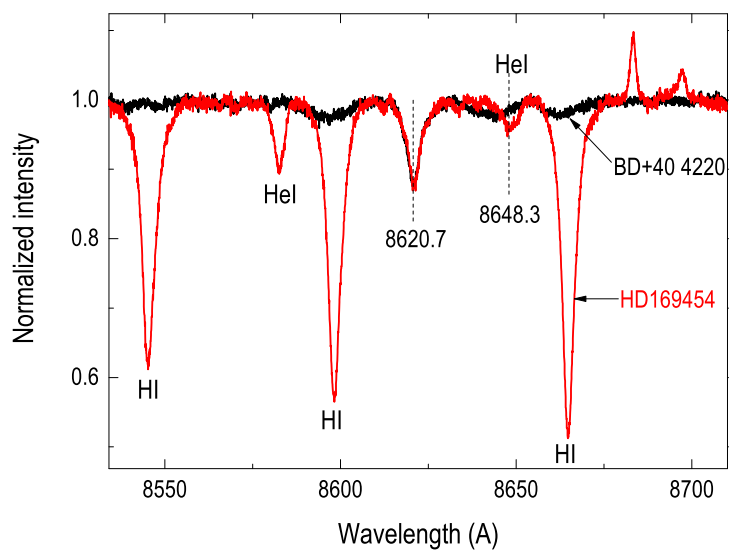


Figure 1: DIB 8620 and stellar lines in the spectra of two heavily reddened stars normalized to the depth of the 8620 DIB. Note the Paschen and HeI lines. The vertical dashed lines indicate the interstellar features, mentioned by Jenniskens & Desert (1994).

line. Munari et al.(2008) mention two HeI lines at 8648.258 Å and 8650.811 Å in the vicinity of the postulated 8648 DIB. Besides, the feature (DIB 8648) does not correlate with reddening. The line is blue-shifted (in the spectrum of BD+40 4220) in relation to the 8620 DIB, which is evident and strong. BD+40 4220 is a heavily reddened, rapidly rotating, very hot star and, therefore, it is very useful to separate stellar and interstellar features. DIB 8620 is relatively broad feature: indeed, its typical full width at the half maximum (FWHM) is about 130 km/s. For example, FWHM of the major DIB 5780 is  $\sim 110$  depending on the line of sight. Hereby, Fig. 1 proves that the DIB 8620 is the only unambiguous broad and strong spectral feature of interstellar origin in the depicted spectral range.

Does the 8620 DIB intensity provide a better estimate of  $E(B - V)$  than other DIBs? The first problem is the spectral range of near-IR. In this range the quantum efficiency of CCD matrices is much lower than in the visual one that makes the S/N ratio lower. Moreover, one can expect some stellar contaminations, especially in the continuum around the 8620 DIB, that is also demonstrated in Fig. 1 of Munari et al.(2008). Owing to the complexity of the 8620 DIB profile, we decided to measure it by an original method developed in DECH package<sup>1</sup>: we have used 8620 DIB observed in the spectrum of the heavily reddened and rapidly rotating object BD+40 4220 as a template. To measure this DIB in other targets we have rescaled manually the depth of the template to match the feature in other targets. BD+40 4220 was observed using the ESPaDOnS spectrograph attached at the 3.6m CFHT. The spectrograph is especially well designed for observations in near-IR range. Since the DIB is broad – its profile is not affected by the Doppler splitting in any object.

Fig. 2 demonstrates how the measurements have been done. The high S/N profile of 8620 DIB (seen in BD+40 4220) was rescaled (made shallower or deeper) to match the same feature observed in other spectra. Fig. 1 shows how it works. Then, the equivalent width of the rescaled template was measured and attributed to the studied target. This allowed us to avoid the influence of stellar contaminations and reduce the noise effects. The 8620 DIB is a broad feature, and its profile shape does not depend on the spectral resolution varying in our sample. The DIB widths and profiles are not exactly constant but they usually do not differ much in cases of broad features, like 8620.

### 3. Observations

Our analyzed data were acquired using the following four échelle spectrographs:

- BOES (Bohyunsan Echelle Spectrograph) of the Korean National Observatory (Kim et al. (2007)) is installed at the 1.8m telescope of the Bohyunsan Observatory in Korea. The spectrograph has three observational modes

---

<sup>1</sup> <http://www.gazinur.com/DECH-software.html>

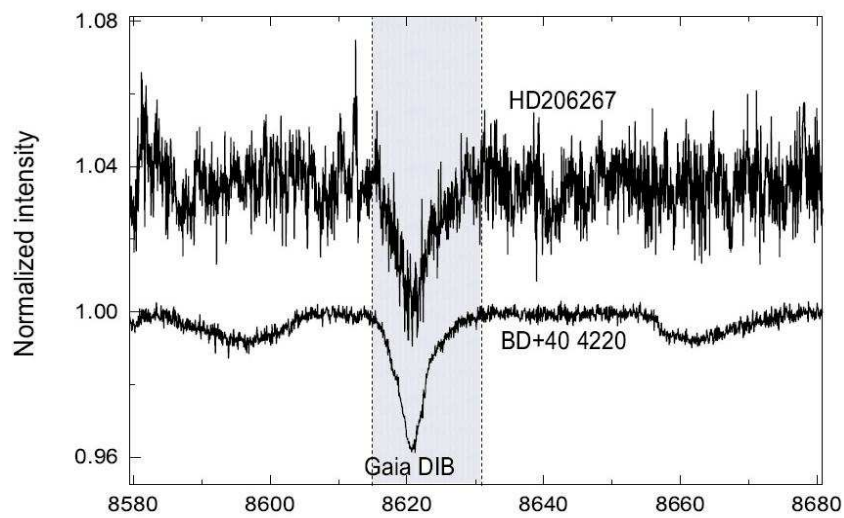


Figure 2: An illustration of the method we have applied for measurements of the equivalent width of 8620 DIB in noisy spectra. Profile of 8620 DIB with a high S/N ratio (seen in BD+40 4220) was rescaled (made more shallow than in the observed spectrum) to match the depth of the same interstellar feature observed in the spectrum of HD206267. Then, the equivalent width of the rescaled template was measured and attributed to the studied target. In the figure, spectra are vertically displaced for clarity.



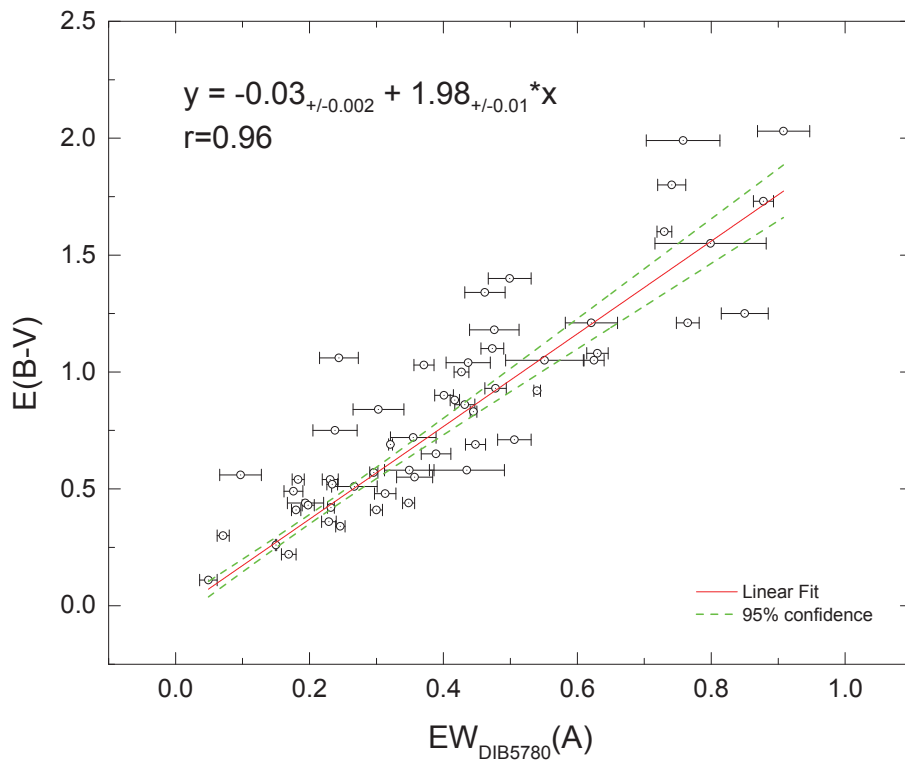


Figure 3:  $EW(5780)$  as the proxy of  $E(B-V)$ . Also in this case (like in Fig. 4) the observed scatter is most likely grounded in physical parameters of the intervening clouds.

allowing resolving powers of 30,000, 45,000 and 90,000. The lowest resolution, which enables observations of rather faint, heavily reddened, distant objects, was used in most of cases. In any mode, the spectrograph covers the whole spectral range from  $\sim 3500$  to  $\sim 10,000$  Å, divided into 75 – 76 spectral orders;

- MAESTRO (MAtrix Echelle SpecTROgraph) is attached to the 2 m telescope at the Terskol Observatory (the North Caucasus). It is a three branch cross-dispersed échelle spectrograph installed at the Coudé focus (F/36) of the telescope. It was designed for stellar spectroscopy using high resolutions from  $R = 45,000$  to 190,000 in the spectral range 3500 – 10000 Å. The lowest resolution mode (sufficient for our programme) allows one to reach spectra of objects as faint as  $\sim 10^m$  with a sufficient ( $\sim 100$ ) signal-to-noise ratio;
- CAFE spectrograph (Calar Alto high-Resolution facility, Southern Spain) fed by 2.2m telescope provides high resolution échelle spectra over 3700–9100 Å. The resolution of the spectrograph is up to  $R = 62,000$ ; the whole range is divided into 92 orders;
- ESPaDOnS spectrograph (Echelle SpectroPolarimetric Device for the Observation of Stars) is the bench-mounted high-resolution échelle spectrograph/spectropolarimeter attached to the 3.58 m Canada-France-Hawaii telescope at Mauna Kea (Hawaii, US). It is designed to obtain a complete optical spectrum in the range from 3,700 to 10,050 Å. The whole spectrum is divided into 40 échelle orders. The resolving power is about 68,000. The ESPaDOnS is especially useful for observations in near-IR since the high altitude of the observatory allows one to minimize the telluric contaminations.

The spectra from BOES were gathered during the period from 2004 to 2015, with PI G. Galazutdinov. The spectra from ESPaDOnS were obtained during the runs 05Ao5 (in 2010, with PI B. Foing) and 15AD83 (in 2015, with PI G. Walker). Spectra from MAESTRO were acquired between 1996 and 2016 by the authors. Spectra from CAFE were collected in February 2007 by Y. Beletsky.

The above mentioned spectra are of various quality, therefore, those which do not allow reliable measurements were not involved in our study. Our sample includes those spectra which mostly have high enough S/N ( $\geq 150$ ) and where the feature at  $\lambda$  8620.7 Å can be reliably traced. All spectra have been reduced by the authors.

#### 4. Results and discussion

We have measured the equivalent widths of the most prominent DIBs at  $\lambda\lambda$  8620.7, 5780.6, 5797.0, 6196.0, 6379.3, and 6613.5 Å, as well as of the two strongest molecular features, namely CH (near 4300.3 Å) and CH<sup>+</sup> (near 4232.5

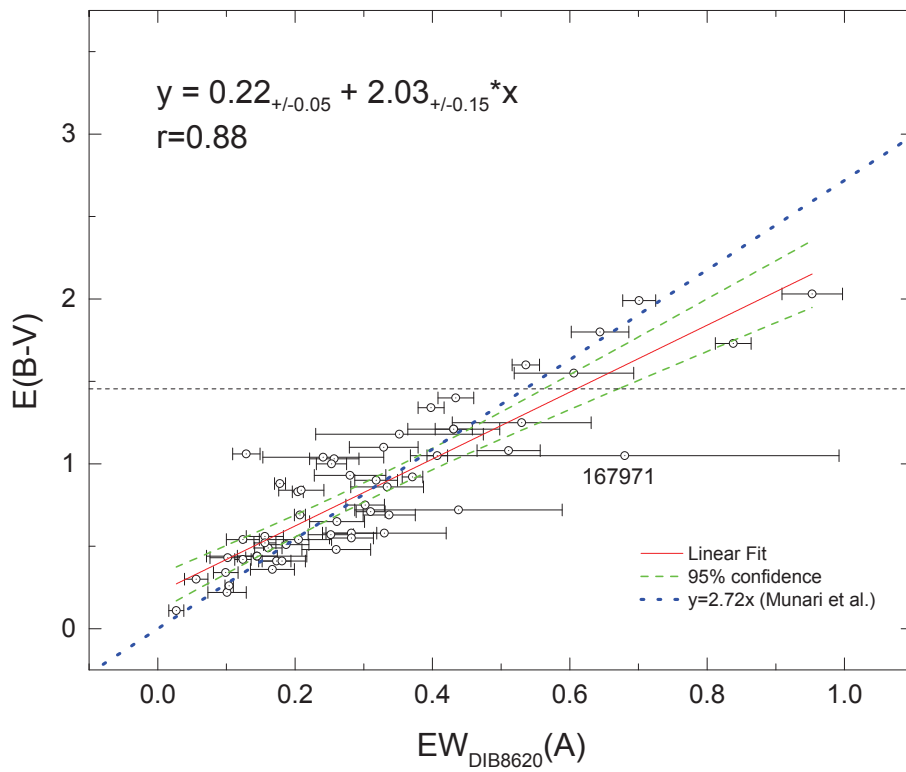


Figure 4:  $E(B - V)$  plotted as a function of  $EW(8620)$  for our sample of spectra. Horizontal dashed line sets the  $E(B - V)$  limit for the sample of Munari et al. (2008); his fit to the depicted points is shown together with ours. (Note: samples are not identical.)

Table 1: Equivalent widths of DIBs and molecules (in mÅ).

Star	$E_{B-V}$	8620	5780	5797	6196	6379	6614	CH, (4300 Å)	CH <sup>+</sup> , (4232 Å)
BD+59451 <sup>b</sup>	0.86	334±53	432±15	134± 5	48± 2	88± 3	182± 5	40.0± 2.0	18.0± 2.0
BD+59456 <sup>b</sup>	0.69	337±38	448±15	121± 6	46± 2	89± 3	202± 8	40.0± 3.0	23.0± 2.0
BD+60594 <sup>b</sup>	0.58	282±37	349±37	138±13	40± 2	69± 2	162± 5	25.0± 2.0	17.0± 1.0
BD+404220 <sup>e</sup>	1.99	701±24	758±55	239±25	96±10	95±10	306±19	78.0± 6.0	86.0± 8.0
BD+582580 <sup>b</sup>	1.08	511±46	630±16	212± 9	82± 2	89± 2	291±11	35.0± 5.0	21.0± 3.0
BD+592735 <sup>b</sup>	1.25	530±101	850±35	282±15	117±10	189±10	424±25	60.4±19.8	45.7±15.4
CygOB2_7 <sup>b</sup>	1.80	644±42	741±21	197±10	89±10	95± 9	327±20	65.5±11.9	93.7±32.6
CygOB2_8A <sup>b</sup>	1.60	536±20	730±11	175± 5	93± 8	88± 5	336±16	43.0± 3.0	83.0± 3.0
CygOB2_11 <sup>b</sup>	1.73	838±26	878±15	179±10	112±16	87± 8	366±22	43.1±12.1	94.5±20.9
CygOB2_12 <sup>e</sup>	2.03	953±44	908±39	330±37	115±19	140±19	391±37	–	–
13256 <sup>b</sup>	1.21	431±67	621±39	223±18	90± 6	93± 6	297±21	46.0± 9.0	–
14956 <sup>b</sup>	0.88	178±8	417± 7	145± 3	45± 1	105± 1	219± 4	37.2± 2.2	26.7± 3.2
15497 <sup>b</sup>	0.83	204±8	445± 5	142± 2	43± 1	65± 2	232± 4	44.5±15.9	60.8±19.4
15785 <sup>b</sup>	0.65	261±40	389±22	150±11	44± 5	96± 5	220±10	26.2± 1.8	23.4± 4.0
21291 <sup>t</sup>	0.44	144±73	194±27	67±13	26± 6	34± 8	95±18	16.1± 4.1	7.2± 2.6
24534 <sup>b</sup>	0.56	156±27	97±31	73± 5	17± 5	56± 8	75±10	23.7± 1.9	3.7± 1.8
31327 <sup>c</sup>	0.54	124±24	183± 9	77± 4	30± 2	70± 4	111± 6	25.7± 5.0	23.3± 6.2
32991 <sup>c</sup>	0.41	173±21	180± 7	68± 3	20± 3	43± 2	68± 4	20.3± 2.3	15.4± 1.8
34078 <sup>e</sup>	0.49	161±20	176±14	57± 6	20± 4	17± 4	70± 9	54.8± 3.9	37.4± 4.2
36371 <sup>c</sup>	0.41	181±34	300± 9	90± 3	38± 2	81± 4	141± 4	16.5± 3.0	15.2± 3.5
36861 <sup>b</sup>	0.11	27±11	49±13	20± 4	5± 2	7± 2	16± 6	1.8± 0.2	0.9± 0.1
41117 <sup>c</sup>	0.44	145±29	348± 9	117± 4	34± 1	64± 2	151± 4	14.0± 2.2	19.9± 6.8
42087 <sup>c</sup>	0.34	99±18	246± 7	95± 4	30± 2	75± 6	105± 4	14.3± 3.9	7.5± 2.8
43384 <sup>b</sup>	0.58	330±90	435±56	130±29	47±12	88±15	199±24	16.1± 6.4	32.0± 8.5
46202 <sup>b</sup>	0.48	260±50	313±16	88± 8	36± 3	52± 3	153±11	15.9± 3.4	15.7± 4.8
145502 <sup>e</sup>	0.22	101±28	169±11	34± 5	16± 3	28± 3	60± 8	3.6± 0.5	6.6± 1.1
147165 <sup>b</sup>	0.36	167±32	229±11	37± 4	18± 1	29± 2	65± 5	3.1± 0.1	5.3± 0.3
147889 <sup>b</sup>	1.03	257±36	371±15	156± 8	34± 3	81± 4	173± 7	49.8± 1.1	27.7± 1.2
147933 <sup>e</sup>	0.43	102±26	198± 9	51± 5	16± 2	28± 3	66± 6	17.9± 0.4	13.1± 1.4
149757 <sup>e</sup>	0.30	56±17	71± 9	33± 3	11± 2	18± 2	44± 4	17.9± 0.1	23.5± 2.1
167971 <sup>t</sup>	1.05	680±312	551±58	163±25	78±24	109± 8	254±28	29.0± 2.0	51.7± 2.8
168607 <sup>b</sup>	1.55	606±87	799±83	261±35	100± 4	159± 2	393±13	47.1± 2.9	73.0± 1.8
169454 <sup>e</sup>	1.10	329±50	473±17	159± 8	61± 6	102± 6	216±17	29.8± 0.5	18.2± 0.4
173438 <sup>b</sup>	1.00	253±22	427±11	209± 8	42± 2	100± 3	229±10	34.0± 3.0	20.0± 2.0
183143 <sup>e</sup>	1.26	431±27	765±17	195± 8	93± 4	111± 5	361±16	38.7± 3.0	49.0± 2.8
185859 <sup>b</sup>	0.57	252±33	296± 6	148± 3	42± 1	142± 5	213± 3	21.0± 1.0	18.0± 2.0
186745 <sup>b</sup>	0.93	280±52	478±16	198± 5	60± 2	139± 2	278± 7	40.0± 2.0	46.7± 5.5
190603 <sup>t</sup>	0.72	438±151	355±34	89±17	36± 8	82±22	109±27	15.2± 1.6	31.4± 2.7
190918 <sup>b</sup>	0.42	124±12	232± 5	58± 4	27± 2	14± 1	92± 4	9.9± 5.8	14.3± 3.1
192163 <sup>b</sup>	0.26	104±6	150± 1	52± 2	26± 1	14± 1	76± 2	7.5± 1.4	17.1± 2.1
193793 <sup>b</sup>	0.69	207±8	321± 3	94± 1	41± 1	32± 1	161± 4	22.4± 2.0	53.4± 8.1
194279 <sup>t</sup>	1.18	352±122	476±37	127±12	58±15	105±10	201±34	33.4± 9.9	47.0±15.9
204827 <sup>b</sup>	1.06	129±20	244±29	187±13	37± 2	91± 1	163± 4	68.7± 3.7	31.9± 3.7
206267 <sup>t</sup>	0.54	205±48	231±12	85± 5	26± 1	40± 3	122± 6	21.0± 1.0	14.0± 1.0
207538 <sup>b</sup>	0.51	187±33	267±34	166±17	33± 1	96± 2	168± 6	30.4± 1.8	7.3± 1.3
208501 <sup>b</sup>	0.75	302±28	238±33	112±20	31± 2	63± 3	113± 4	37.0± 4.2	12.6± 5.2
210839 <sup>t</sup>	0.53	156±16	234± 8	78± 3	31± 1	53± 2	140± 4	21.4± 1.9	9.3± 0.4
217035 <sup>b</sup>	0.71	310±21	506±25	142±10	50± 2	88± 2	211± 6	27.0± 2.0	25.0± 1.0
217086 <sup>t</sup>	0.92	371±15	540± 5	156± 2	59± 2	87± 2	266± 4	39.0± 3.0	44.1± 4.0
219287 <sup>b</sup>	1.05	407±15	625±15	166± 7	81± 2	73± 2	261± 7	33.0± 3.0	21.5± 2.0
226868 <sup>b</sup>	0.90	318±31	401±14	125± 5	45± 2	68± 2	171± 4	41.0± 2.0	51.0± 2.0
228712 <sup>b</sup>	1.34	398±19	462±30	123±12	57± 7	57± 5	189±15	37.0± 1.0	34.0± 2.0
228779 <sup>b</sup>	1.40	434±26	499±32	194±14	62± 1	106± 2	268± 6	54.4± 6.6	51.1± 13.6
235825 <sup>b</sup>	0.55	282±32	357±27	98±15	28± 2	52± 3	134± 4	9.8± 4.9	7.0± 2.4
254577 <sup>b</sup>	1.04	241±88	437±33	145±14	52± 6	84± 5	208±13	38.6± 6.2	30.3± 8.0
281159 <sup>b</sup>	0.84	209±33	303±38	99±15	31± 2	56± 2	152± 6	40.0± 2.0	38.0± 1.0

Å), in the spectra of 56 reddened stars, which are distributed around the Milky Way disc. As mentioned, our sample includes only spectra with  $S/N \geq 150$ .

All the measurements of equivalent width and color excess  $E(B - V)$  are collected in Table 1. Here, letters ‘b’, ‘c’, ‘e’, and ‘t’ stand for BOES, CAFE, ES-PaDOnS, and MAESTRO spectrographs, respectively.  $(B - V)$ ’s of selected targets were taken from the SIMBAD database; their intrinsic values allowed us to calculate color excesses  $E(B - V)$  (see Papaj et al.(1993)).

Comparison of our values of  $E(B - V)$  and EW, calculated for DIBs at  $\lambda$  5780.6, 5797.0, 6196.0, and 6613.5 Å, with those presented in Friedman et al.(2011) indicates that both sets sufficiently agree. The relation between  $EW(5780)$  and  $E(B - V)$  given by Friedman et al.(2011) (the correlation coefficient is  $r=0.82$ ) agrees with our one ( $r=0.96$ ) (Fig. 3) proxy inside the calculated errors. The differences of  $0.01 - 0.05$  in  $E(B - V)$  are probably due to spectral stellar classification errors. A nearly systematic mismatch for EWs at  $\lambda$  5797.0 Å (namely, Friedman’s values are larger than ours) is caused by inclusion in measurements of the blue wing or rather the additional DIB at  $\lambda$  5795 Å, the latter being correlated rather with the neighbouring 5780 DIB than with 5797 DIB. This is a good example of the risk of using measurements from different sources for a compilation.

We used the results obtained (and presented here for the first time) to check the relation between  $EW(8620)$  and  $E(B - V)$  reported by Munari et al.(2008). Our project is the first one based on high resolution spectra. Fig. 4 depicts  $E(B - V)$  plotted as a function of  $EW(8620)$  for our sample of spectra. Our relation is reasonably similar to that of Munari et al.(2008) but some differences bring one to a number of questions: Is the observed scatter a result of measurement errors? Or the fact that we used another sample of objects plays an important role? And is the 8620 DIB a unique feature, especially tightly related to  $E(B - V)$ ?

Toward answering these questions, we shall expound below our findings, based upon an analysis of both 8620 DIB and some other DIBs.

Fig.5 demonstrates the same parts of two spectra acquired using the BOES spectrograph of the Korea National Observatory. Both objects are almost identically reddened. However, 8620 DIB is  $\sim 2.5$  times stronger in BD+58 2580. It is a matter of fact that the observed intensities of 8620 DIB can be different in spectra of objects with the same  $E(B - V)$ . This resembles the behaviour of the (similarly broad) 5780Å DIB reported by Krelowski & Westerlund (1988). Therefore, the scatter, which is seen in Fig. 4, apparently follows physical differences between intervening clouds. It thus suggests that using  $EW(8620)$  to estimate  $E(B - V)$  in any individual case may be risky. In fact, a very similar relation between equivalent width and colour excess may be found for another broad DIB, namely 5780 DIB (Fig. 3).

A relation between  $EW(5780)$  and  $E(B - V)$  was recently published by Raimond et al.(2012). Their relation, which suffers a very broad scatter (their Fig. 3), is somewhat different than that of us. It is very likely an effect of using nearby,

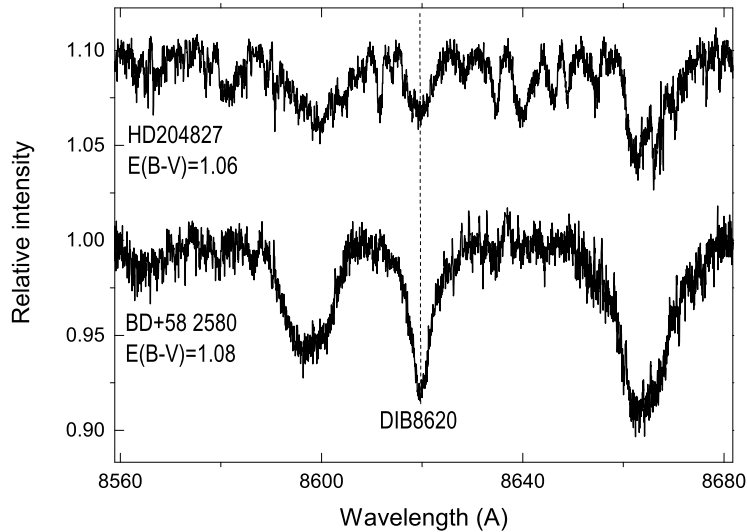


Figure 5: Spectra (parts) of two identically reddened stars with the marked 8620 DIB. The great apparent difference of the DIB's strengths is evident.

mostly late B type stars. Likely while considering relatively nearby objects the inhomogeneity of the interstellar medium plays an important role. In such cases an DIB intensity can hardly play the role of  $E(B - V)$  proxy.

Raimond et al.(2012) calculated the distances from the Hipparcos trigonometric parallaxes, given in the SIMBAD database. These parallaxes are, likely in many cases, incorrect due to large errors. For instance, the authors give the distance to HD165052 as big as 6667 pc. The Gaia DR1 parallax of HD165052 is  $0.66 \pm 0.31$  mas that leads to a distance of 1515 pc. The new Gaia DR2 one is  $0.78 \pm 0.05$  that leads to the distance of 1280 pc. It seems worth of being mentioned that our method, based on interstellar CaII line intensities (Megier et al. 2005), gives a distance 1250 pc to the same star.

Limiting the range of  $EW(5780)$  to a more narrow one led to the higher scatter. For example, in Fig. 3 of Friedman et al.(2011), where the scatter is quite high, the  $E(B - V)$  range is limited within 0 - 0.7 mag only. Our Fig.3 shows a much lower scatter while the  $E(B - V)$  is in the range 0-2.0.

The spectra of Friedman et al.(2011) show examples of extra strong (in comparison to  $E(B - V)$ ) 5780 DIBs ( $\sigma$ Sco) or to the opposite case (HD53367). The scatter observed is caused by different physical properties of individual clouds. In cases of a broad  $E(B - V)$  range, the individual differences become negligible in relation to  $E(B - V)$  and thus the correlation starts looking tight. However, applying such average relation to individual objects is ill-recommended. These examples

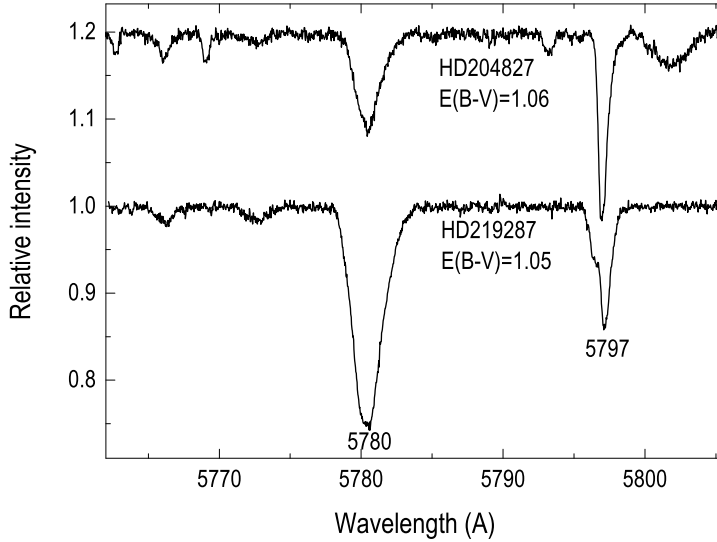


Figure 6: The strength ratio of two major DIBs: 5780 and 5797 may be of evidently different strength ratio in two objects of identical reddening.

confirm the early result of Krelowski & Westerlund (1988). Our relation proves that 5780 DIB is as good a proxy of  $E(B - V)$  as the Gaia DIB. Longer sightlines likely intersect many clouds and thus one observes in every case an ill-defined average; such averages are similar if the number of intersected clouds is large (Krelowski & Strobel (2012)). This is why the correlation between DIB intensities and  $E(B - V)$  is tighter for distant objects and why DIB intensities are risky  $E(B - V)$  proxies in cases of nearby stars.

Plain evidence of this fact can be found in Fig. 6 where spectra of two different stars are shown. It seems to be interesting that 5780 DIB, which is rather broad, is relatively weak in the spectrum of HD204827 while the narrow 5797 DIB is especially strong. This resembles the  $\zeta$  and  $\sigma$  type clouds, first mentioned by Krelowski & Westerlund (1988), and HD219287 resembles the  $\sigma$  case. It is to be mentioned that the 8620 DIB behaves in unison with the 5780 DIB, which is similarly broad.

DIBs are commonly believed to be carried by some interstellar molecules. However, the molecular species, identified in translucent clouds, where DIBs are observed, are usually just diatomics; the strongest features belong to CH and  $\text{CH}^+$ . Are the latter related to  $E(B - V)$ ? Fig. 7 demonstrates that individual relations between reddening and strength of molecular features (e.g.  $\text{CH}^+$ ) may differ from object to object. Apparently, simple interstellar molecules behave in translucent clouds in the same fashion as diffuse band carriers. However, it does not mean

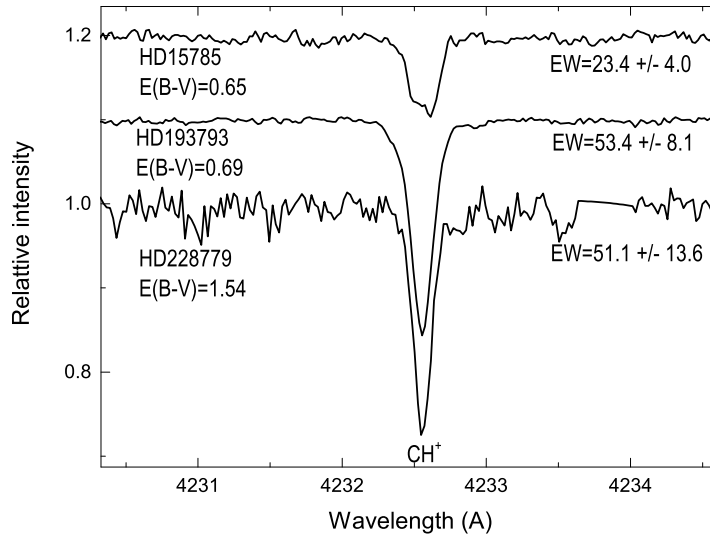


Figure 7: Intensities of diatomics may be different with the same  $E(B - V)$  or identical with different  $E(B - V)$ .

that the behavior of the latter allows one to predict that of simple molecules. For instance, the spectrum of HD204827, where 5780 DIB is very weak, contains extra strong CH lines (like in any  $\zeta$  case). We also demonstrated recently (Krelowski et al. 2019) that  $CH^+$  lines can be strong (in the Pleiades cluster) while all DIBs are barely visible.

Finally, we have analyzed the correlations of intensities of several reasonably strong DIBs to  $E(B - V)$ . Figs. 3 and 4, as well as Fig. 8 demonstrate that in cases of practically all diffuse bands and features of simple diatomic molecules, one can build correlations which are of similar correlation coefficients. The Gaia DIB does not seem to be an exclusive case. Almost every other interstellar spectral features, only if measured precisely enough, can be used to estimate  $E(B - V)$  with a similar accuracy (and risk). The correlation looks poor in the case of the 6379 DIB. This is most likely because of the contaminating stellar nitrogen line, which is difficult to be properly removed even in our high resolution spectra. In the case of low resolution, the separation is entirely impossible.

## 5. Conclusions

In our research, we used 56 OB stars to measure intensities of several DIBs in order to check their correlation with color excess  $E(B - V)$ . It is appropriate to mention here that the relation between reddening and equivalent width of DIBs has



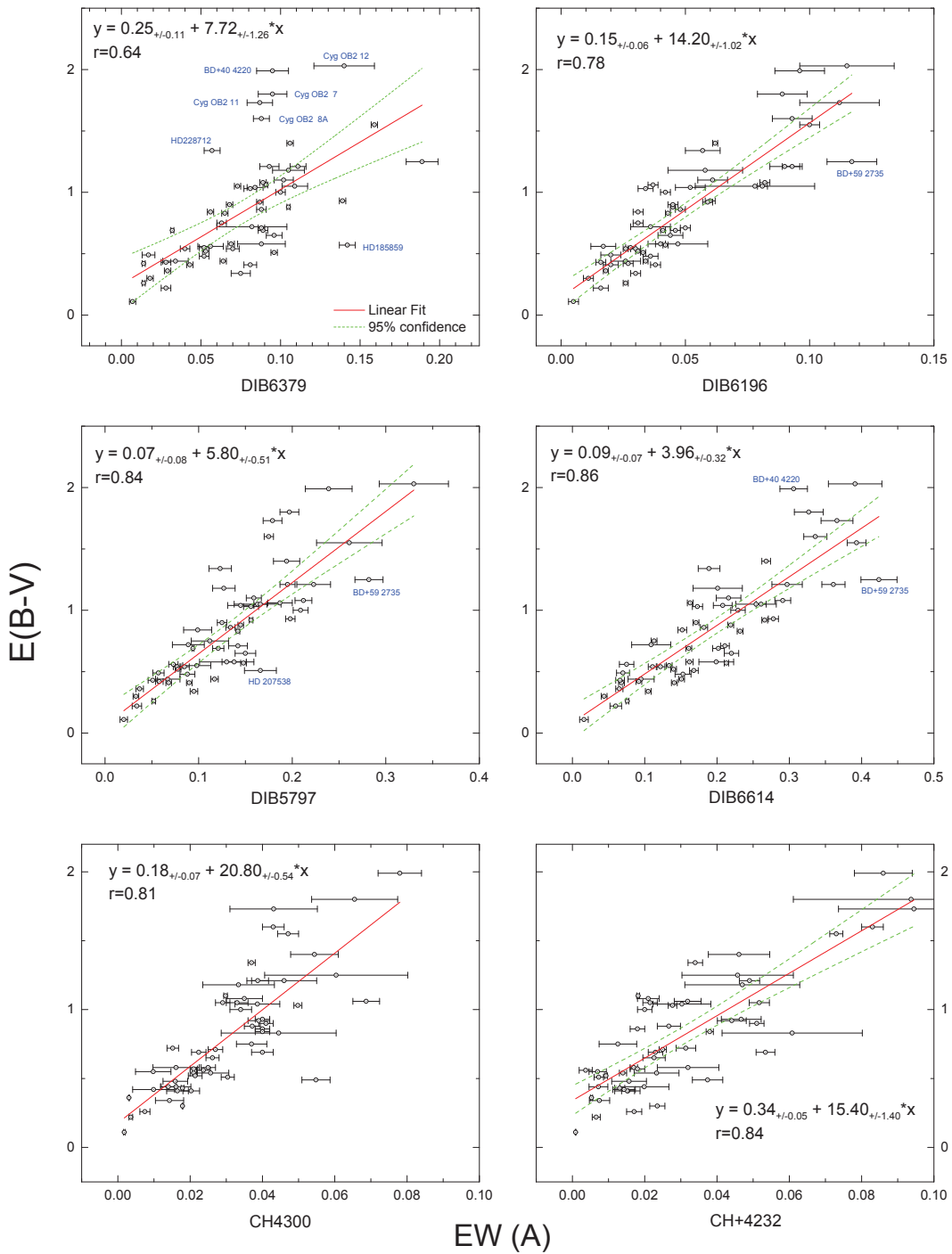


Figure 8: Correlation between  $E(B-V)$  and equivalent widths of several DIBs and molecular lines of simple diatomics. The correlations, except for 6379 DIB (see text), look very similar.

been studied for a long time. In particular, Munari et al.(2008) proposed to use the 8620 DIB as a tool to estimate reddening of stars. This diffuse interstellar band at  $\lambda$  8620.7 Å is the only unambiguous one, which falls into the spectral range of the Gaia RVS spectrometer.

A major conclusion of our analysis is that DIB carriers are in a way related to dust grains (spatial correlation?) but none shows a very tight relation. The 8620 DIB is of importance for observations with Gaia, but the 5780 DIB gives a similarly accurate  $E(B - V)$  proxy. It must be emphasized that an estimate of reddening, based on any interstellar spectral feature, may be incorrect, despite the rather tight correlation between any of the interstellar lines/bands and  $E(B - V)$  if the range of the latter is broad. Our fits of straight lines were done without fixing the intercepts. Anyway, the calculated intercepts are nearly zero indeed. Only in the case of the  $\text{CH}^+$  line (Fig. 8) we observe the intercept as big as 0.35. Actually, the line is observed in practically zero reddening (e.g. in Pleiades). Apparently, the existing fits depend on the samples selected. On the other hand, the fact that all interstellar features do correlate tightly with reddening may suggest that the carriers of all these lines/bands/extinction are (in average) reasonably well mixed in all interstellar clouds. Thus, the observations of identified features of interstellar molecules can be used to estimate physical properties of clouds and analyze their influence on diffuse band carriers only in cases of targets being obscured by single absorption clouds. Since the latter differ from object to object we observe a very similar scatter of physical origin in any sample of similar  $E(B - V)$ . Only adding such “boxes” we get a correlation. Thus the correlations between different DIBs and  $E(B - V)$  look tight in cases of a broad range of extinction, most likely caused by many clouds along any line-of-sight. Apparently, such average relations allow estimates of  $E(B - V)$ 's from intensities of interstellar spectral features only in cases of high values of  $E(B - V)$ 's originated in several clouds each. High extinction, single cloud objects (like HD204827) are evident outliers from the average relation.

The above considerations lead to the following conclusions:

- intensities of all DIBs (not only those of the 8620 DIB) are correlated to a similar degree with  $E(B - V)$ ;
- the above relation is valid if a large diversity of interstellar clouds is averaged. Individual clouds may be peculiar but only these peculiarities can be physically interpreted;
- the scatter observed in our plots is of physical origin. This is why we observe tight correlations only in cases of broad ranges of  $E(B - V)$ 's resulting from adding up the optical depths of several (many) clouds; this confirms the conclusions of Bailey et al. (2016) and earlier publications on the subject;
- only in the above mentioned cases (high  $E(B - V)$ 's, many clouds) intensities of DIBs, in particular of the Gaia DIB at  $\lambda$  8620.7 Å, may serve as an extinction proxy.

**Acknowledgements.** JK acknowledges the financial support of the Polish National Science Centre (the grant UMO-2017/25/B/ST9/01524 for the period 2018—2021). Polish and Ukrainian authors benefited from the funds of the Polish-Ukrainian PAS/NASU joint research project (2018 – 2020). GG and JK acknowledge the support of CONICYT program "REDES Internacionales" project REDES180136.

## REFERENCES

- Campbell E. K., Holz M., Gerlich D., Maier J. P. 2015, *Nature*, **523**, 322.  
 Campbell E. K., Holz M., Maier J.P., Gerlich D., Walker G.A.H., Bohlender D. 2016, *ApJ*, **822**, 17.  
 Campbell E. K., Holz M., Maier J. P. 2016, *ApJ*, **826**, L4.  
 Cordiner, M. A. et al. 2019, *ApJ*, **875**, 28.  
 Daminieli A. et al. 2016, *MNRAS*, **463**, 2653.  
 Fan H., Hobbs L.M., Dahlstrom J.A., Welty D.E., York D.G., Rachford B., Snow T.P., Sonnentrucker P., Baskes N., Zhao G. 2019, *ApJ*, **in press**, .  
 Field G.B. 1974, *ApJ*, **187**, 453.  
 Fitzpatrick E.L., Massa D. 2007, *ApJ*, **663**, 320.  
 Friedman S.D. et al. 2011, *ApJ*, **727**, 33.13  
 Galazutdinov, G. A., Musaev, F. A., Krelowski, J., Walker, G. A. H. 2000, *PASP*, **112**, 648.  
 Galazutdinov G.A., Lee Jae-Joon, Han Inwoo, Lee Byeong-Cheol et al. 2017, *MNRAS*, **467**, 3099.  
 Galazutdinov, G. A., Shimansky, V. V., Bondar, A., Valyavin, G., Krelowski, J. 2017a, *MNRAS*, **465**, 3956.  
 Galazutdinov, G. A., Krelowski, J. 2017b, *Acta Astronomica*, **67**, 159.  
 Greenstein J.L. & Aller L.H. 1950, *ApJ*, **111**, 328.  
 Hamano S., Kobayashi Na., Kondo S., Sameshima H. et al. 2016, *ApJ*, **821**, 42.  
 Hartmann J. 1904, *ApJ*, **19**, 268.  
 Heger M.L. 1922, *Lick Obs.*, **10**, 141.  
 Hobbs L.M., York D.G., Snow T.P., Oka T. et al. 2008, *ApJ*, **680**, 1256.  
 Jenniskens P. & Desert F.-X. 1994, *A&A*, **106**, 39.  
 Kashuba S.V. et al. 2016, *MNRAS*, **461**, 839.  
 Kerr T.H., Hibbins R.E., Fossey S.J., Miles J.R. & Sarre P.J. 1998, *ApJ*, **495**, 941.  
 Kim K.-M., Han I., Valyavin G.G., Plachinda S. et al. 2007, *PASP*, **119**, 1052.  
 Kos J. et al. 2013, *ApJ*, **778**, 86.  
 Kos, J. et al. 2014, *Science*, **345**, 6198.791  
 Krelowski J. 2018, *PASP*, **130**, 1001.  
 Krelowski J. & Strobel, A. 2012, *AN*, **333**, 60.  
 Krelowski J. & Westerlund B.E. 1988, *A&A*, **190**, 339.  
 Krelowski, J., Strobel, A., Galazutdinov, G. A., Bondar, A., Valyavin, G. 2019, *MNRAS*, **486**, 112.  
 Maíz Apellániz J., Barbá R.H., Sota A., Simón-Díaz S. 2015, *A&A*, **583**, 132.  
 McKellar A. 1941, *PASP*, **53**, 233.  
 Megier A. et al. 2005, *ApJ*, **634**, 451.  
 Merrill P.W., Wilson O.C. 1938, *ApJ*, **87**, 9.  
 Moutou, C., Krelowski, J., D’Hendecourt, L., and Jamroszczak, J. 1999, *A&A*, **351**, 680.  
 Munari U. et al. 2008, *A&A*, **488**, 969.  
 Papaj J., Krelowski J., Wegner W. 1993, *A&A*, **273**, 575.  
 Raimond S., Lallement R., Vergely J. L., Babusiaux C. & Eyer L. 2012, *A&A*, **544**, 13.  
 Siebenmorgen R., Voshchinnikov N. V. & Bagnulo S. 2014, *A&A*, **561**, A82.  
 Sneden C., Wozczyk A. & Krelowski J. 1991, *PASP*, **103**, 1005.  
 Trumpler R.J. 1930, *PASP*, **42**, 214.

- Wallerstein G., Sandstrom K., Gredel R. 2007, *PASP*, **119**, 861.  
York B. et al. 2014, *Proc. IAUS No. 297*, **2013**, (J.Cami & N.L.J.Cox, eds.)